2022 IEEE 25th International Conference on Intelligent Transportation Systems (ITSC)
October 8-12, 2022, Macau, China

General Driving Behavior Model based on the Desired Safety Margin for Vehicle Flow Simulation

Pinlong Cai[1], Junjie Zhang[2], Xuan Zhao[1], Yikang Li[1,*]

Abstract— **Traffic flow simulation is indispensable for the construction of digital urban traffic. Similar-to-real simulation can provide an effective verification platform for intelligent traffic managements. Traffic flow simulation includes complex vehicle behavior modeling, trajectory estimation and planning. This paper establishes a general driving behavior model that is applied in car-following, lane-changing and merging scenarios. The general driving behavior model consists of three parts. First, the initial and terminal conditions of trajectories are determined according to different driving purposes, and they are used for trajectory planning based on a cubic polynomial fitting method. Second, the geometric coupling relationship among vehicles' expected trajectories are analyzed. Third, the active risk perception process based on the desired safety margin is used to determine the best choice of optional trajectories. The proposed general driving behavior model is validated by real traffic flow data, and then some statistical analysis results of traffic parameters show that the proposed model performs much better than the baseline model.**

I. INTRODUCTION

The research on traffic flows in urban roads and highways has always been a focus in traffic field. Traffic flow is a macroscopic traffic phenomenon composed of the movement of vehicles or others, which reflects the operation of road traffic with a series of microscopic and macroscopic traffic parameters [1]. With the development of computer science and other technologies, more and more scholars pay attention to using mathematical and physical models to reproduce the dynamic change process in the actual transportation system [2], [3], that is, traffic flow simulation. Traffic flow simulation can analyze the evolution of macroscopic traffic states with the help of microscopic behavior modeling and provide supports for modern intelligent traffic managements with numerical calculation or statistical analysis results. Vehicle flow studied in this paper is the most common traffic flow.

Car-following motion in vehicle flow is the simplest vehicle behavior. A car-following process refers to a scenario that a vehicle follows its front vehicle in a single lane, and the following vehicle velocity is adjusted according to the velocities and positions of two vehicles. The car-following models have been studied for over 60 years [4]–[14]. Gazis et al. proposed the Gazis-Herman-Rothery (GHR) model considering velocity, relative velocity, and headway [6], and many researchers devoted to calibrating the parameters and validate the GHR model by real data [7]. Bando et al. proposed the optimized velocity model and they assumed that car-following processes are based on drivers' desires to maintain the optimal velocities in traffic streams [8]. Subsequently, Jiang et al. overcame the disadvantages of the optimized velocity model and it was further extended to the full velocity difference (FVD) model [10]. Treibe et al. proposed an intelligent driver model (IDM) that is widely used in vehicle flow simulation because it has fewer parameters to be determined [12], whereas the human interference is not considered in the IDM model. Based on the risk homeostasis theory, Lu et al. proposed a desired safety margin (DSM) model with different physiological and psychological characteristics of drivers, which can describe drivers' reactions to active risk perceptions well [13], [14]. Subsequently, the DSM model is used to analyze the stability and safety in the car-following process [15], [16].

Lane-changing motion is another common vehicle behavior, whereas it is more complex than car-following motion, because it is related to not only longitudinal motions but also lateral motions. A classic lane-changing model is MOBIL (minimizing overall braking induced by lane change) proposed by Kesting et al., which derives discretionary and mandatory lane-changing rules based on car-following models [17]. The MOBIL model just gives the intentions of lane-changing motions according to the optional longitudinal accelerations, whereas the lane-changing trajectories need to be optimized by other methods. Similar lane-changing intention inference methods can be found in recent research [18]. To provide the effective and safe trajectories, some researchers try to use optimal control theory to solve the lane-changing motion planning task [19]. However, the optimization methods require a lot of numerical calculations, so it is suitable for providing guidance for automatic vehicles, but not for describing the behaviors of many human-driving vehicles in the real vehicle flow.

Generally, drivers have systematic perceptions, judgments, and executions to control the vehicles. The DSM model provides a novel idea to analyze the risk perceptions of drivers when they make decisions. However, the DSM model just analyzes longitudinal motion of the two successive vehicles, which can be seen a special case of two-dimensional plane motions of vehicles. For two-dimensional plane motions, the trajectory planning is necessary, and the risk perceptions affect behavioral decision-making processes. Although the behavior model considers a driver's reaction time, the output frequency of the model decision is too high to truly reflect the driver's actual decision-making process. To describe the human-like driving behaviors and realize similar-to-real vehicle flow simulation, this paper

[1]Shanghai AI Laboratory, Shanghai 200232, China
[2]Hefei Innovation Research Institute of Beihang University, Hefei 230012, China
*Corresponding Author: Yikang Li, e-mail: liyikang@pjlab.org.cn

2022 IEEE 25th International Conference on Intelligent Transportation Systems (ITSC) | 978-1-6654-6880-0/22/$31.00 ©2022 IEEE | DOI: 10.1109/ITSC55140.2022.9922057

proposes a general driving behavior model based on the desired safety margin (GDBDSM). In the proposed model, a real-time trajectory planning method is used to provide multiple choices at each decision-making process, including car-following, lane-changing, merging, and other reasonable but arbitrary behaviors. Then, the desired safety margins are affected from the relative positions and motion statuses of surrounding vehicles, which provide drivers with the determinants of optimal trajectory selection. Finally, according to the real data collected by the NGSIM program, the proposed general driving behavior model is validated with the statistic characteristics of traffic parameters, and it is compared with the baseline model.

The contributions of this paper include three points as below.

(1) The arbitrary two-dimensional trajectory planning with a cubic polynomial fitting method for vehicles is realized, and then the vehicle interaction mechanism is decoupled by the kinematic and geometric analysis.

(2) The desired safety margin theory is extended from car-following scenarios to general scenarios, and it supports to optimal trajectory selection at each decision-making process.

(3) On the basis of the desired safety margin theory, the GDBDSM model integrating perception, estimation and decision-making is realized for the similar-to-real vehicle flow simulation.

The rest of this paper is organized as follows. Section II presents the two-dimensional trajectory planning method for multiple vehicle behaviors. Section III extends the desired safety margin theory for the optimal trajectory selection. Section IV introduces the vehicle flow simulation. Section V concludes this study and gives some perspectives for future application.

II. TRAJECTORY PLANNING FOR MULTIPLE VEHICLE BEHAVIORS

A. Determination of the Initial and Terminal States

Many driving behavior models have high frequency to give model outputs in decision-making processes, and such outputs are used to describe the drivers' operations of the controlled vehicles. Actually, the decision-making cycle should not be less than drivers' reaction time, except in emergencies. Moreover, at each decision-making process, the drivers always plan the vehicle trajectories in the next period of time, which is the planning time length defined by T. Dislike many existed behavior models, the planning time length should be long enough to complete specific motions. The trajectory planning method is introduced here.

The Cartesian coordinate system is established to describe the motion states of vehicles. A state is defined by $S = \{x, y, v, \theta\}$, where x, y, v, and θ represent the horizontal coordinate, the vertical coordinate, the velocity, and the leading angle, respectively.

The trajectory planning process of any vehicle first needs to determine its initial state and terminal state. The initial state is defined by $S_0 = \{x_0, y_0, v_0, \theta_0\}$, and the terminal state is defined by $S_t = \{x_t, y_t, v_t, \theta_t\}$. As the definition above, the planning time length from S_0 to S_t is T. The premise of trajectory planning is the driver's perception of the surrounding traffic state. Because of the reaction time, the start time of planning should be later than perception. Thus, the initial state is the state of the vehicle the reaction time after the perception.

The terminal states are related to driving purposes. Considering car-following, lane-changing, merging, and other behaviors, the terminal states have different cases. In the car-following scenario, the vehicle is always consistent with the center line of the current lane. Normally, the vehicle also can change the lane and arrive at the center lines of two adjacent lanes. Thus, there are three lateral displacements in three cases. We assume that the vehicle travels with approximately uniform acceleration in a short time, so the longitudinal displacement depends by the terminal velocity v_t. According to kinematic formulas, Eq. (1) can be obtained.

$$\begin{cases} v_t = v_0 + a \cdot T \\ s = \dfrac{1}{2}(v_0 + v_t)T \end{cases} \tag{1}$$

where a is the acceleration and s is the longitudinal displacement. The different selection of a leads to different optional trajectories.

B. Trajectory Fitting by Cubic Polynomial Curves

According to the initial state and the terminal state, the trajectory can be fitted by two cubic polynomial curves to ensure the continuity of motion in horizontal and vertical dimensions. The related motion parameters are displacements, velocities in two dimensions. The velocity is decomposed according to the leading angles θ_0 and θ_t as Eq. (2).

$$\begin{cases} v_0^x = v_0 \cdot \cos(\theta_0) \\ v_0^y = v_0 \cdot \sin(\theta_0) \\ v_t^x = v_t \cdot \cos(\theta_t) \\ v_t^y = v_t \cdot \sin(\theta_t) \end{cases} \tag{2}$$

Then, the kinematic relations among displacements, velocities, and time for the planning trajectory are shown in Eq. (3).

$$\begin{cases} v_t^x = 3a_1T^2 + 2b_1T + v_0^x \\ v_t^y = 3a_2T^2 + 2b_2T + v_0^y \\ x_t = a_1T^3 + b_1T^2 + v_0^xT + x_0 \\ y_t = a_2T^3 + b_2T^2 + v_0^yT + y_0 \end{cases} \tag{3}$$

where a_1, a_2, b_1, and b_2 are coefficients. To solve these coefficients, Eq. (3) can be rewritten and solved in the vector form shown in Eq. (4)-(6).

$$P = \begin{pmatrix} 3T^2 & 2T & 0 & 0 \\ 0 & 0 & 3T^2 & 2T \\ T^3 & T^2 & 0 & 0 \\ 0 & 0 & T^3 & T^2 \end{pmatrix} \tag{4}$$

$$B = \begin{pmatrix} v_t^x - v_0^x \\ v_t^y - v_0^y \\ x_t - (x_0 + v_0^xT) \\ y_t - (y_0 + v_0^yT) \end{pmatrix} \tag{5}$$

$$A = P^{-1}B = (a_1, b_1, a_2, b_2)^T \tag{6}$$

At each decision-making process, the driver can get an expected trajectory for the next planning time length. The decision-making cycle (the time gap between two decision-making processes) is subject to the reaction time, which is usually less than the length of a planning time length. Thus, a specific vehicle movement behavior, such as a lane-changing behavior, needs several decision-making and execution processes. If there is an emergency, the driver may change the original decision and adjust the previous expected trajectory.

C. Selection for the Optimal Trajectory

As the analysis above, at each decision-making process, there are many optional trajectories. Considering the constrains by the desired safety margin, introduced in Section III, some optional trajectories would be abandoned. For the rest of optional trajectories, the drivers can choose one according to their preferences. Under normal circumstances, the drivers always prefer the trajectory that has the terminal state with the farthest longitudinal displacement (i.e., the maximum terminal velocity) and the smallest lateral displacement. Fig. 1 shows an example about the selection for optimal trajectory. The priority order of five trajectories is as follows: *Trajectory 2* $>$ *Trajectory 3* $>$ *Trajectory 5* $>$ *Trajectory 1* $=$ *Trajectory 4*.

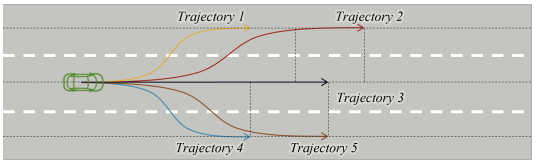

Fig. 1. An example of selection for the optimal trajectory.

Drivers generally tend to drive smoothly in the current lane unless they feel a very uncomfortable driving experience (another vehicle with a low velocity in front is common) or they encounter an intersection. To avoid the negative impact of frequent lane-changing behaviors on vehicle flow, a buffer of lane-changing intention is added. Such a buffer is used to record the drivers' intentions to change lanes. For example, the initial value of the buffer is zero; at each decision-making process, if the trajectory for changing the lane to left is the optimal choice, then the buffer value plus one; otherwise, if the trajectory for changing the lane to right is the optimal choice, then the buffer value minus one. Only the absolute value of the buffer is large than the predefined threshold, and then the drivers will take practical actions to change the lane to left or right. Because the lane-changing motion needs several decision-making and execution processes to be completed, when the vehicle is changing the lane to the left, it can no longer change to the right unless the vehicle reaches the center line of the target lane. A similar restriction on changing the lane to the right also exists.

III. DESIRED SAFETY MARGIN FOR TRAJECTORY SELECTION

A. Trajectory Conflict Discrimination by Geometric Analysis

Before the decision-making process, the drivers need to perceive the surrounding traffic states first. In this paper, we set a perception distance for drivers. A perception cycle takes the ego vehicle's position as the center and the perception distance as the radius. All the other vehicles within the cycle are concerned in the risk perception model. According to the states of the other vehicles, drivers can roughly estimate their trajectories of a planning time length. Subsequently, drivers need to judge whether the ego vehicles will have conflicts with any other vehicles, that is, whether the expected trajectories of the ego vehicles will intersect with the trajectories of any other vehicles. The discrimination process is shown in Fig. 2.

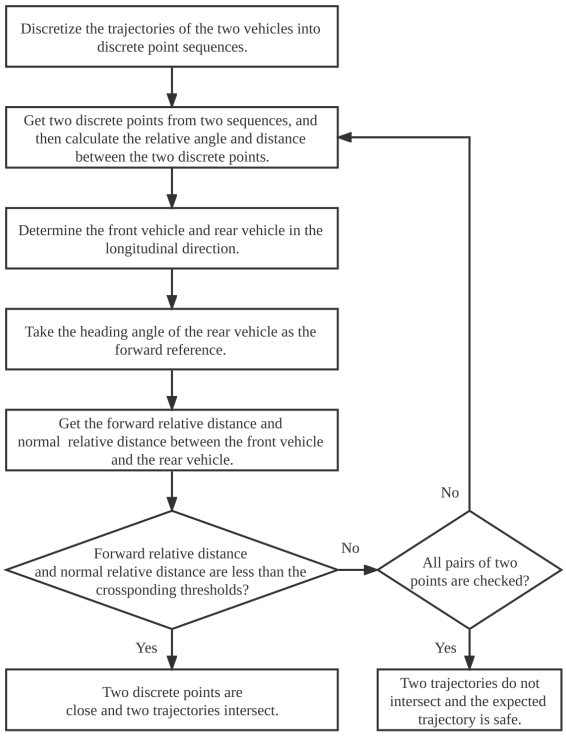

Fig. 2. Trajectory conflict discrimination process.

At first, the trajectories of the two vehicles are discretized into two discrete point sequences. Then, we get two of discrete points $S_1(x_1, y_1, v_1, \theta_1)$ and $S_2(x_2, y_2, v_2, \theta_2)$ from two sequences, and then calculate the relative angle and distance between the two discrete points, and determine the front vehicle and the rear vehicle in the longitudinal direction according to the positions of the two vehicles. The equations of the relative angle R_a and the relative distance R_d are shown in Eq. (7).

$$\begin{cases} R_a = \arctan((x_2 - x_1)/(y_2 - y_1)) \\ R_d = \sqrt{(x_2 - x_1)^2 + (y_2 - y_1)^2} \end{cases} \tag{7}$$

Next, we take the heading angle of the rear vehicle as the reference of forward direction. In order to determine the relative position of the front vehicle, R_d is projected to the forward direction and the normal direction (perpendicular to forward direction) of the rear vehicle according to R_a. If the forward relative distance is less than the predefined safety distance threshold in longitudinal direction $Safe_x$ and the normal distance is less than the other predefined safety distance threshold in lateral direction $Safe_y$, then the two discrete points are close, that is, two trajectories intersect. Finally, when all pairs of two points are far away, the expected trajectory is safe.

When two trajectories intersect, because the estimated trajectory of the other vehicle is not accurate enough, the other vehicle may occupy the other positions in the expected trajectory of the ego vehicle. Considering the discrete point sequence of the ego vehicle, the driver need to determine whether the other vehicle can occupy any point before the ego vehicle. According to the Dubins curves [20], the shortest distance between these discrete points and initial state of the other vehicle can be calculated, defined by d_k^*. Then, if Eq. (8) is satisfied, then the other vehicle can occupy k point first and the driver will perceive active risk with the other vehicle.

$$t_k + t_r + t_d > d_k^*/v^* \tag{8}$$

where t_k is the time required for the ego vehicle to reach kth point, t_r is the reaction time of the driver, t_d is the decision-making cycle, v^* is the velocity of the other vehicle.

B. General Desired Safety Margin

According to the analysis above and referring to the DSM model used in car-following [13], [14], the active risk ξ_k at kth point (latent conflict position) can be defined in Eq (9), related to the displacement during reaction time δ_r, the displacement during decision-making cycle δ_r, the inertia displacement of the ego vehicle δ_i, the inertia displacement of the other vehicle δ_i^*, and the minimum relative distance from current position to the latent conflict position δ_k.

$$\xi_k = (\delta_r + \delta_d + \delta_i - \delta_i^*)/\delta_k \tag{9}$$

$$\delta_r = v_k t_r \tag{10}$$

$$\delta_d = v_k t_d \tag{11}$$

$$\delta_i = v_k^2/2a_m^- \tag{12}$$

$$\delta_i^* = \pm(\lambda v^*)^2/2a_m^- \tag{13}$$

where v_k is the velocity at this point, a_m^- is the maximum of the deceleration, and λv^* is the component of velocity v^* of the other vehicle along the tangent direction of the expected trajectory of the ego vehicle. $\lambda \in [0, 1]$, which is determined by the difference between the leading angles of the ego vehicle and the other vehicle. When the component of velocity v^* of the other vehicle has the same direction with the expected state of the ego vehicle at the latent conflict position, the inertia displacement value of the other vehicle is greater than 0; Otherwise, it less than 0 and the perceived risk is high. Fig. 3 is the schematic diagram of this process.

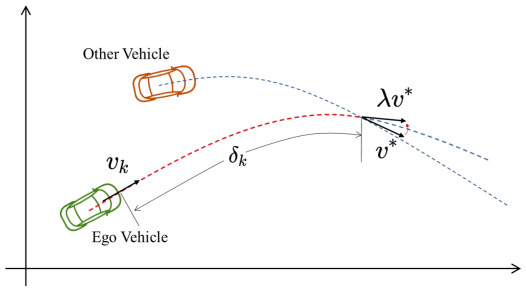

Fig. 3. The calculation of active risk between two vehicles.

Due to the rough estimations about the other vehicles, the perceived risks are dynamic when the ego vehicle follows the expected trajectories. The divers can adjust their expected trajectories to handle with sudden risks. For example, when an ego vehicle cannot complete the lane-changing motion because its expected trajectory is suddenly occupied by the other vehicle, and then the ego vehicle should be able to return to the original lane if it has no other choices. Thus, besides the other vehicles that have latent conflicts with the ego vehicle, the front vehicle in the original lane always needs to be considered to ensure the ego vehicle can move safely in the original lane. The active risk between two vehicles in the same lane is similar to the DSM model.

Based on the active risk ξ, the general desired safety margin is defined as below.

$$\zeta = 1 - \exp(-\hat{\xi}) \tag{14}$$

where $\hat{\xi}$ is limited by the cut off values on both sides of ξ, $0 \leq -\hat{\xi} \leq M$, and M is a large positive number. Thus, the range of the general desired safety margin ζ is 0 to 1. The general desired safety margin decreases with the increase of planning time length, which reflects that drivers tend to be be more conservative for the longer future. Thus, at the begin of the planning trajectories, the safety margins must be larger than the minimum of safety threshold. At the end of the planning trajectories, the safety margins must be larger than the maximum of safety margin threshold. The thresholds at other points are obtained by linear interpolation, and the safety margin of other points in the trajectories must be greater than its corresponding thresholds.

IV. SIMULATION AND VALIDATION

A. Real Data from the NGSIM program

The Next Generation SIMulation (NGSIM) program collected detailed and high-quality traffic datasets to support the research of microscopic driver behaviors. In this paper, we try to simulate the road segment (shown in Fig. 4) with busy traffic statuses presented in the Interstate 80 (I-80) freeway dataset. The dataset includes three 15-minute periods. The time of period 1 is from 4:00 p.m. to 4:15 p.m. The time of period 2 is from 5:00 p.m. to 5:15 p.m. the time of period 3

is from 5:15 p.m. to 5:30 p.m. More details about the dataset can refer to the homepage [21].

The traffic demands of all lanes (six lanes and an onramp located within the study area) in three 15-minute periods are referred in the simulations. The numbers of vehicles of all lanes are shown in TABLE I.

TABLE I

THE NUMBERS OF VEHICLES IN 15-MINUTE PERIODS.

Lane ID	1	2	3	4	5	6	7
Period 1	239	247	194	247	228	228	147
Period 2	273	253	208	221	237	243	188
Period 3	376	199	178	174	205	191	190

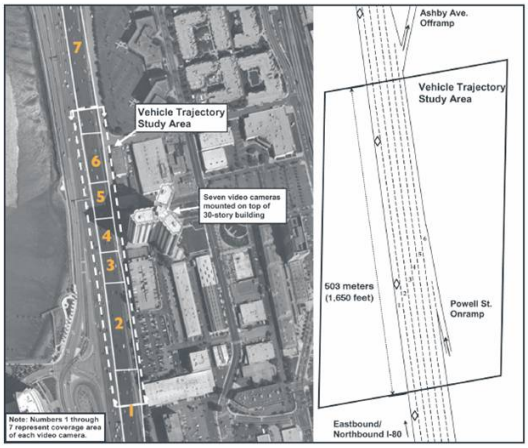

Fig. 4. The study area on eastbound I-80 in the San Francisco Bay area, Emeryville, CA.

B. Simulations and Comparisons

The self-developed simulation platform based on the PyGame modules of Python is used for vehicle flow simulations. The geometric lines of the road segment are drawn according to Fig. 4. We simulate the vehicle flows during three periods. The flows of real data provide the arrival time and initial velocities to create vehicle objects at the beginning of the road segment, and then vehicles run on the road segment following the proposed GDBDSM model. In the simulations, vehicles can not only run along straight lines but also change lanes to run more smoothly and get higher velocities. Moreover, vehicles from the onramp can merging into the main road. The model parameters in the simulations are shown in TABLE II.

The baseline model combined by the IDM model and the MOBIL model is used for comparisons. In such a model, the vehicles can follow their front vehicles by following the IDM model, and the MOBIL model offers the intentions for lane-changing behaviors. The lane-changing trajectories are fitted by frequently-used fifth order Bezier curves.

The comparisons of velocity distributions are shown in Fig. 5. The blue lines are generated by the real data. The orange and green lines are the simulation results of

TABLE II

PARAMETERS AND SETTINGS.

Parameter Description	Setting
Length of road segment	503 m
Width of lane	3.75 m
Reaction time	0.5 s
Decision-making cycle	0.5 s
Safety distance threshold in longitudinal direction	8 m
Safety distance threshold in lateral direction	3 m
Maximum of safety margin threshold	0.6
Minimum of safety margin threshold	0.3
Maximum of expected velocity	20 m/s
Perception distance	50 m

the GDBDSM model and the baseline model, respectively. The orange lines are closer to the blue lines compared to the green lines, which reflects that the GDBDSM model simulates better to describe the vehicle flows in the real data. The Kullback–Leibler (KL) divergence is selected as the measure to quantify velocity distribution differences, and detailed values are shown in TABLE III. Compared to the baseline model, the KL divergences in our model are reduced by 99.9%, 99.6%, and 98.6% in period 1, period 2, and period 3, respectively. A video of the simulation at period 1 by the GDMDSM model is provided in this link: https://www.bilibili.com/video/BV1Am4y1d7WT/.

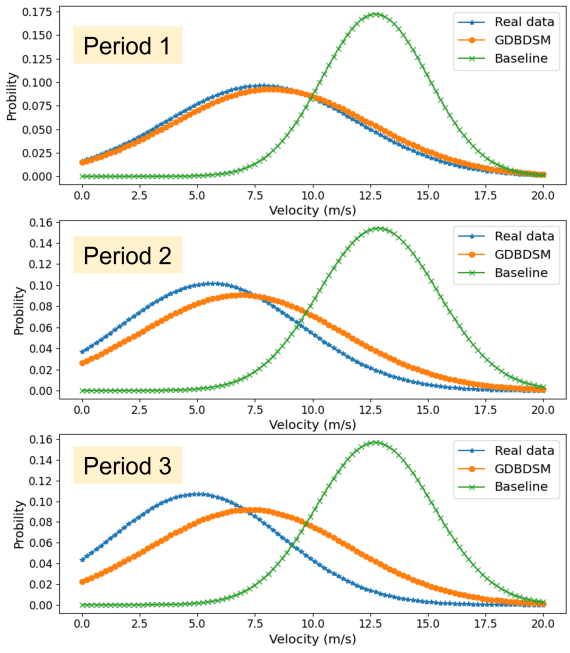

Fig. 5. Comparisons of velocity distribution curves.

Then, we try to study the macroscopic traffic characteristics in the vehicle flow simulations. Plenty of studies show that the macroscopic fundamental diagram exists in urban traffic based on experimental data or simulation models [22]. It can describe the relationship between flows and densities and reflect the traffic dynamics. Here, we calculate the traffic

TABLE III

KL DISTANCES BETWEEN SIMULATION AND REAL DATA.

Periods	Period 1	Period 2	Period 3
Baseline	1.1936	1.5562	1.7219
GDBDSM	0.0007	0.0070	0.2418

demands per hour by the numbers of vehicles at period 1. The traffic demands of all lanes are four times of the value in the TABLE I. We set the coefficients ranging from 0.0 to 2.0 to generate different demands in the study area. The time of each simulation is 100 s, of which 50 s for warming up the simulations. The vehicle count point is set at the position that is 50 meters to the end of the road segment. In each simulation, the numbers of vehicles passing through the vehicle count point are used to calculate the flows, and the numbers of vehicles in the road segment at the end time of simulations are used to calculate the densities. In Fig. 6, the macroscopic fundamental diagram is given to present the relationship between flows and densities. With the increase of densities, the flows first increase and then decrease, which are consistent with the real traffic phenomenons.

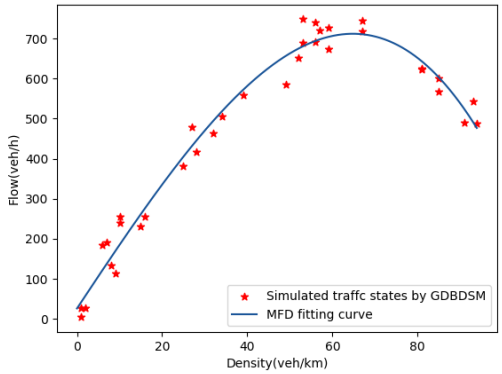

Fig. 6. Macroscopic fundamental diagram generated by the GDBM model.

V. CONCLUSIONS

To describe the human-like driving behaviors, this paper proposes the GDBDSM model used for car-following, lane-changing, and merging scenarios. The cubic polynomial curves are used to get optional trajectories with the terminal states given according to different driving purposes. The desired safety margin theory is extended to determine whether latent conflicts exist or not among trajectories. The proposed model well explains the overall strategies of drivers' risk perception and trajectory planning.

Referring to the NGSIM dataset, this paper realizes the similar-to-real vehicle flow simulation by the self-developed simulation platform based on PyGame. From the comparisons about velocity distributions of the simulation results, the GDBDSM model outperforms the baseline model combined by the IDM model and the MOBIL model. The macroscopic fundamental diagram shows the simulations by the GDBDSM model are consistent with real traffic dynamics.

In the future, the proposed model can be applied to the simulation of local road network to study the management and control model of road network. Moreover, the proposed model can support the generation of near real vehicle flows for the simulation tests of autonomous vehicle models, so as to improve the test efficiency.

REFERENCES

[1] D. L. Gerlough and M. J. Huber, Traffic flow theory, Transp. Res. Board Special Report, 1976.

[2] L. E. Owen, Y. Zhang, L. Rao, and G. McHale, Traffic flow simulation using CORSIM, IEEE Winter Simul. Conf. Proc., pp. 1143-1147, Dec. 2000.

[3] K. Nagel, P. Wagner, and R. Woesler, Still flowing: Approaches to traffic flow and traffic jam modeling, Oper. res., vol. 51, no. 5, pp. 681-710, 2003.

[4] L. A. Pipes, An operational analysis of traffic dynamics, J. Appl. Phys., vol. 24, no. 3, pp. 274–281, 1953.

[5] R. E. Chandler, R. Herman, and E. W. Montroll, Traffic dynamics: Studies in car following, Oper. Res., vol. 6, pp. 165–184, 1958.

[6] D. C. Gazis, R. Herman, and R. W. Rothery, Nonlinear follow-theleader models of traffic flow, Oper. Res., vol. 9, no. 4, pp. 545–567, 1961.

[7] P. Ranjitkar, T. Nakatsuji, and A. Kawamua, Car-following models: An experiment based benchmarking, J. Eastern Asia Soc. Transp. Stud., vol. 6, pp. 1582–1596, 2005.

[8] M. Bando, K. Hasebe, A. Nakayama, A. Shibata, and Y. Sugiyama, Dynamical model of traffic congestion and numerical simulation, Phys. Rev. E, Stat. Phys. Plasmas Fluids Relat. Interdiscip. Top., vol. 51, no. 2, p. 1035, 1995.

[9] G. E. Farin and D. Hansford, Generalized force model of traffic dynamics, Phys. Rev. E, Stat. Phys. Plasmas Fluids Relat. Interdiscip. Top., vol. 58, pp. 133–138, 1998.

[10] R. Jiang, Q. Wu, and Z. Zhu, Full velocity difference model for a car-following theory, Phys. Rev. E, Stat. Phys. Plasmas Fluids Relat. Interdiscip. Top., vol. 64, p. 017101, 2001.

[11] X. Zhao and Z. Gao, A new car-following model: Full velocity and acceleration difference model, Eur. Phys. J. B, Condens. Matter Complex Syst., vol. 47, pp. 145–150, 2005.

[12] M. Treiber, A. Hennecke, and D. Helbing, Congested traffic states in empirical observations and microscopic simulations, Phys. Rev. E, Stat. Phys. Plasmas Fluids Relat. Interdiscip. Top., vol. 62, no. 2, pp. 1805, 2000.

[13] G. Lu, B. Cheng, Q. Lin, and Y. Wang, Quantitative indicator of homeostatic risk perception in car following, Safety Sci., vol. 50, no. 9, pp. 1898–1905, 2012.

[14] L. Li, G. Lu, Y. Wang, and D. Tian, A rear-end collision avoidance system of connected vehicles, Proc. IEEE Int. Conf. Intell. Transp. Syst., pp. 63–68, 2014.

[15] J. Zhang, Y. Wang, and G. Lu, Impact of heterogeneity of car-following behavior on rear-end crash risk, Accident Anal. & Prevention, vol. 125, pp. 275-289, 2019.

[16] J. Zhang, G. Lu, H. Yu, Y. Wang, and C. Yang, Effect of the uncertainty level of vehicle-position information on the stability and safety of the car-following process, IEEE Trans. Intell. Transp. Syst., early access, DOI: 10.1109/TITS.2020.3044623, 2020.

[17] A. Kesting, M. Treiber, and D. Helbing, General lane-changing model MOBIL for car-following models, Proc. Transp. Res. Board, pp. 86–94, 2007.

[18] J. Wang , Z. Zhang , and G. Lu, A Bayesian inference based adaptive lane change prediction model, Trans. Res. C, Emerg. Technol., vol. 132, pp. 103363, 2021.

[19] L. Bai , Y. Zhang , Y. Ge , Z. Shao, and P. Li, Optimal control-based online motion planning for cooperative lane changes of connected and automated vehicles, IEEE/RSJ Int. Conf. Intell. Robots Syst., 2017.

[20] L. E. Dubins, On curves of minimal length with a constraint on average curvature, and with prescribed initial and terminal positions and tangents, AM. J. MATH., vol. 79, no. 3, pp. 497-516, 1957.

[21] NGSIM, Next Generation Simulation, URL: https://ops.fhwa.dot.gov/trafficanalysistools/ngsim.htm, 2006.

[22] L. Zhang, Z. Yuan, L. Yang, Z. Liu, Recent developments in traffic flow modelling using macroscopic fundamental diagram, Transport Reviews, vol. 40, no. 6, pp. 689-710, 2020.